Centerline Formulation in the Numerical Computation of Axisymmetric Flows

Peter C. Sukanek*
Clarkson College of Technology, Potsdam, N.Y.
and
Robert P. Rhodes†
ARO, Inc., Arnold AFS, Tenn.

Nomenclature

a = parameter defined in Eq. (3)
b = Prandtl number for turbulent diffusion
C_μ = constant in effective viscosity relation
F = dependent variable of interest
k = turbulence kinetic energy
m = index of radial point in finite-difference grid
n = index of axial point in finite-difference grid
P = production term in conservation equation
r = radial position
u = axial velocity
v = radial velocity
x = axial distance
Δx = increment in axial distance
ϵ = turbulence energy dissipation
ψ = stream function
μ = effective turbulent viscosity
ρ = density
ω = turbulence vorticity

Subscripts

o = centerline
$+$ = position in finite-difference grid halfway between centerline and first radial location

I. Introduction

THE calculation of most turbulent flows of interest requires numerical computations. This procedure introduces another dimension of uncertainty into the predictions. Errors can arise because of inadequate turbulence models and/or incorrect empirical constants in addition to an improper finite-difference formulation of the governing equations. The purpose of this Note is to illustrate one type of numerical error.

In the calculation of axisymmetric flows, the centerline can be formulated in two different manners. Some investigators[1,2] have chosen to express the governing equations as limiting forms on the centerline. Others[3] find the appropriate finite-difference equations by integrating over the grid interval, thereby avoiding the problem of the indeterminacy of the diffusion term.

While it may seem that either method is acceptable, we will show that for compressible flows and certain types of effective viscosity models, the use of a limiting form of the governing equations can lead to significant errors in the results.

II. Analysis

The equations of conservation of linear momentum, energy, or species mass for an axisymmetric jet with the usual boundary-layer simplification can be written in the form:

$$\frac{\partial F}{\partial x} = \frac{1}{\psi}\frac{\partial}{\partial \psi}\left(\frac{a}{b}\frac{\partial F}{\partial \psi}\right) + P \tag{1}$$

where ψ is the stream function defined as:

$$\psi \frac{\partial \psi}{\partial r} \equiv \rho u r \qquad \psi \frac{\partial \psi}{\partial x} \equiv -\rho v r \tag{2}$$

and F is the appropriate dependent variable, x is the axial distance, P is a production term, b is an appropriate Prandtl number, and

$$a \equiv \mu \rho u r^2 / \psi \tag{3}$$

where μ is the effective viscosity.

Equations of the form of Eq. (1) can also be written for turbulence kinetic energy and turbulence energy dissipation if these quantities are used in the definition of μ.

A number of finite-difference formulations can be used to put Eq. (1) into a form suitable for digital computation. Away from the centerline there are no problems; however, at the centerline, the diffusion term is indeterminate and is often replaced by

$$\left.\frac{\partial F}{\partial x}\right|_{\psi=0} = \left(\frac{2\mu_o}{b}\frac{\partial^2 F}{\partial \psi^2}\right)\Bigg|_{\psi=0} + P_{\psi=0} \tag{4}$$

An alternate formulation of the difference equations involves first integrating the governing equations from the centerline to the radial position halfway between the centerline and the first grid point.

In both cases, the finite-difference representation of Eq. (1) at radial positions other than the centerline is:

$$F_{n+1,m} = F_{n,m} + \frac{\Delta x}{2\psi_m \Delta\psi^2 b}\Big\{(a_{n,m+1}+a_{n,m})(F_{n,m+1}-F_{n,m}) - (a_{n,m}+a_{n,m-1})(F_{n,m}-F_{n,m-1})\Big\} + \frac{\Delta x}{(\rho u)_{n,m}} P_{n,m} \tag{5}$$

The indices (n,m) refer to the axial and radial grid locations. At the centerline, the limiting form of the governing equations results in a finite-difference equation of the form:

$$F_{n+1,0} = F_{n,0} + \frac{4\mu_{n,0}\Delta x}{b(\Delta\psi)^2}(F_{n,1}-F_{n,0}) + \frac{\Delta x}{(\rho u)_{n,0}} P_{n,0} \tag{6}$$

The procedure of integrating the equation gives, at the centerline,

$$F_{n+1,0} = F_{n,0} + \frac{8a_+}{\Delta\psi^2 b}(F_{n,1}-F_{n,0}) + \frac{\Delta x}{(\rho u)_{n,0}} P_{n,0} \tag{7}$$

where a_+ is the average value of the parameter a between the centerline and first-radial grid point.

The first formulation, i.e., treating the centerline by a limiting form of the governing equation, represents the center of the flow as a singularity. The second formulation couples the centerline to the remainder of the flowfield. The distribution of grid points and the dependent variable for both methods is illustrated in Fig. 1.

Comparison of Eqs. (6) and (7) shows that the two differ only in the coefficient of the diffusion term. If the ratio of these coefficients is defined as:

$$R \equiv \mu_o \Delta\psi / 2a_+ \tag{8}$$

Received March 14, 1978; revision received June 26, 1978.

Index category: Jets, Wakes, and Viscid-Inviscid Flow Interactions.
*Assistant Professor, Dept. of Chemical Engineering.
†Research Engineer, Engine Test Facility. Member AIAA.

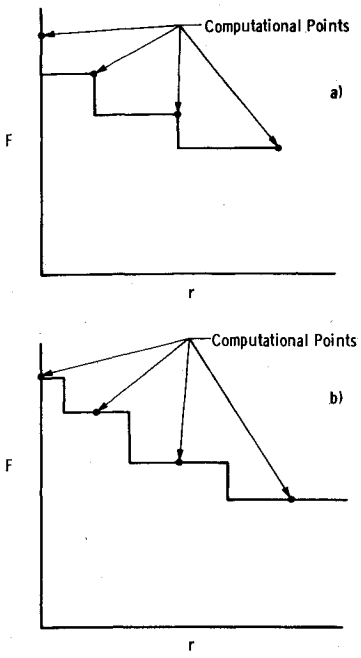

Fig. 1 Grid points and dependent variables with a) Eq, (6) and b) Eq. (7).

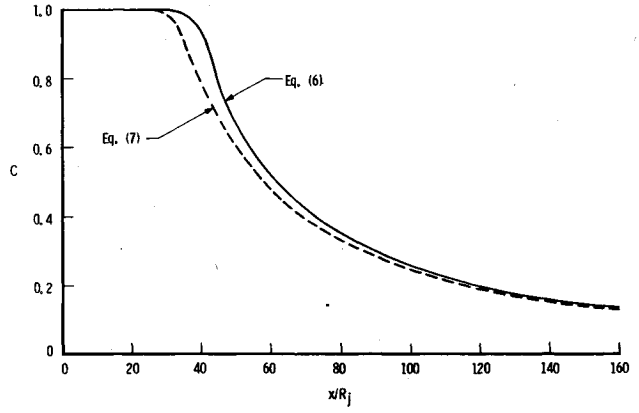

Fig. 2 Centerline species concentration with Eq. (6) (——) and Eq. (7) (---).

it is straightforward to show, using the definition of a, that

$$R=\mu_o/\mu_+ =2\mu_o/(\mu_o+\mu_l) \tag{9}$$

The two formulations will lead to different results if the effective viscosity on the centerline is different from that at the first radial position. The difference between these values depends on the nature of the flow (incompressible or compressible) and on the type of effective viscosity model employed. Since the turbulence viscosity is proportional to the density, the effect should be observed mostly in compressible flows where density variations exist in the radial direction.

III. Results

A number of turbulence models and flowfields were examined. For most combinations, the effect of the specific type of centerline formulation has an insignificant effect on the predictions. There is, however, one important exception: the use of a two-equation turbulence kinetic energy (TKE) model, such as the k-ϵ or k-ω model,[4] to predict the behavior of compressible flow.

The input conditions for the flowfield chosen are given in Table 1. The k-ϵ two-equation TKE model, with an empirical correction for compressibility effects,[5] was used to calculate the flowfield. The predictions of the dimensionless centerline species concentration and the radial distribution of dimensionless concentration at 40 exit radii from the nozzle are shown in Figs. 2 and 3. In both cases, the initial number of grid points for the finite-difference scheme was 13.

Table 1 Input parameters for flowfield calculation

	Jet	Edge
Temperature, K	1300	230
Velocity, m/s	3658	914
Mole fraction, N_2	0.713	0.79
Mole fraction, O_2	0.186	0.21
Mole fraction, He	0.10	0.0

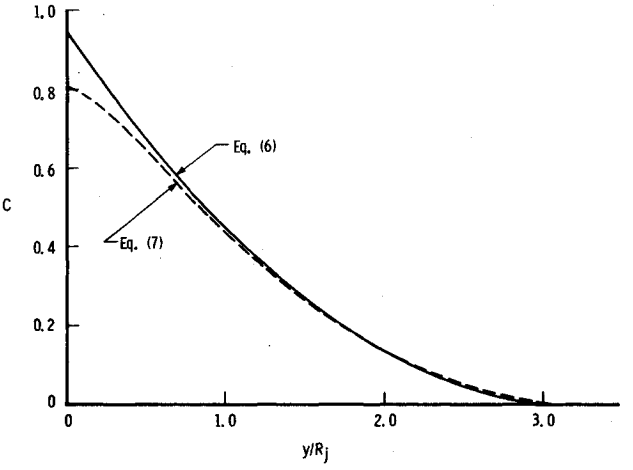

Fig. 3 Radial profiles of species concentration at $x/R=40$ using Eq. (6) (——) and Eq. (7) (---).

It is apparent from the figures that the uncoupled centerline formulation of Eq. (6) predicts a longer core length and consistently higher centerline concentrations than does the coupled formulation of Eq. (7). In addition, the radial profiles are spiked much more at the centerline in the former case. Indeed, the concentration distribution in this case is reminiscent of the qualitative sketch of Fig. 1a.

The reason for the discrepancy in these two cases has to do with the effective viscosity model. In the k-ϵ model, differential equations of the form of Eq. (1) must be written for the turbulence kinetic energy k and the dissipation rate ϵ. As with the other dependent variables, the diffusion of k and ϵ depends on the value of the turbulent viscosity, μ. However, μ is defined as:

$$\mu=C_\mu \rho k^2/\epsilon \tag{10}$$

On the flow centerline, the values of k, ϵ, and μ are isolated, to a large extent, from the remainder of the flow. Since, in the initial portion of the jet, the value of k is low at the centerline, the viscosity is also low there. It increases by the diffusion of the turbulence from the shear layer. If Eq. (6) is used, the diffusion will be small, since μ at the centerline is small. Hence, it takes a longer time for centerline viscosity to increase than if Eq. (7) were employed.

The viscosity ratio R, given by Eq. (9), varies throughout the flowfield. In the calculations presented here, R starts at 1.0 and reaches a minimum value of approximately 0.25 at a dimensionless axial distance (x/R_j) of about 34. It then increases rapidly to a value of 0.97 at 48 radii downstream and approaches 1.0 asympotically. At 40 radii, where the concentration profiles are shown in Fig. 3, the value of R is 0.525.

Since an analytical solution to the problem is not available, the "true" solution cannot be unequivocally identified. However, as the number of grid points in the finite-difference scheme is increased, the predictions using the limiting form at

the centerline, Eq. (6), approach those obtained using Eq. (7). Also, since the latter formulation does not contain the unrealistic uncoupling of the centerline from the remainder of the flow, the "true" solution can be approximated with fewer grid points when the integrated approach is used.

Acknowledgment

This work was performed in part while P. C. Sukanek was a USAF-ASEE Summer Faculty Research Fellow at the Arnold Engineering Development Center. The authors appreciate the sponsorship of this program by the Air Force Office of Scientific Research and its administration by Auburn University.

References

[1]Mikatarian, R. R., Kau, C. J., and Pergament, H. S., "A Fast Computer Program for Nonequilibrium Rocket Plume Predictions," Air Force Rocket Propulsion Laboratory Tech. Rept. AFRPL-TR-72-94, 1972.

[2]Thomas, P. D. and Wilson, K. H., "Efficient Computation of 'Stiff' Chemically Reacting Flow in Turbulent Free Jets," *AIAA Journal*, Vol. 14, May 1976, pp. 629-636.

[3]Jensen, D. E. and Wilson, A. S., "Prediction of Rocket Exhaust Flame Properties," *Combustion and Flame*, Vol. 25, Jan. 1975, pp. 43-55.

[4]Launder, B. E. and Spalding, D. B., *Lectures in Mathematical Models of Turbulence*, Lecture 5, Academic Press, London, 1972.

[5]Dash, S., Weilerstein, G., and Vaglio-Lauren, R., "Compressibility Effects in Free Turbulent Shear Flows," Air Force Office of Scientific Research Tech. Rept. AFOSR-TR-1436, 1975.

Laser-Induced Impulse to a Phenolic Surface

Peter K. Wu* and Peter E. Nebolsine†
Physical Sciences Inc., Woburn, Mass.

Introduction

THE phenomenology of laser-induced impulse to a surface has been studied both in vacuum and under atmospheric conditions.[1,2] This Note examines the transient momentum transfer in vacuum to graphite and carbon phenolic surfaces for laser intensities below the threshold for plasma formation. In vacuum, experimental measurements[3] indicate that the laser-induced breakdown above the carbon phenolic and ATJ graphite surfaces for 10.6μ laser beam is of the order of 10^7 W/cm^2. Here we consider intensities below this level.

Analysis

A one-dimensional transient heat conduction problem has been formulated and applied to carbon phenolic.[2] Here we apply the same analysis to ATJ graphite as well as a carbon phenolic with different characteristics from that of Ref. 2. The nominal resin content in the present carbon phenolic is about 34% by weight while the previous carbon phenolic has a resin content of about 11%. Here we consider the absorption coefficient for 10.6μ to be 0.62 (Ref. 4), instead of 0.81 (Ref. 2) and use a more recent reaction rate for the pyrolysis.[5] Finally, in Ref. 2, the molecular species coming off the surface in the process of vaporization is assumed to be carbon (C). However, recent experiments[6] indicate that C_3 is the predominant specie in the saturated vapor. In these calculations, the thermodynamic properties of both ATJ graphite and carbon phenolic are taken from Ref. 7.

Received April 18, 1978; revision received July 7, 1978.

Index categories: Lasers; Heat Conduction.

*Principal Scientist. Member AIAA.

†Principal Scientist.

The laser energy is assumed to be instantaneously absorbed at the surface. This implies that the absorption length in the solid is small compared with the characteristic thermal depth. For the carbon phenolic, which is made with a carbon fiber content of about 66% by weight and ATJ graphite, the surface absorption assumption is justified because of short absorption depth of 10.6μ radiation in carbon ($\sim 1\mu$).[3] For the carbon phenolic, which is made with a nominal resin content of 34% by weight, the phenolic resin decomposes at an elevated temperature that is below the sublimation temperature of carbon and the phenolic gas is assumed to be able to escape through the porous carbon char.

The calculation of impulse delivered per unit of incident energy, i.e., the "coupling coefficient," requires some knowledge of the conditions above the solid surface. Assuming that the vapor temperature immediately above the surface is the same as the surface temperature, $T_v = T_s$; that the rate of graphite evaporation equals the rate of condensation under equilibrium conditions; and that the accommodation coefficient is unity; one then has the Knudsen-Langmuir expression for vacuum environment

$$P_v = \dot{m}\sqrt{2\pi R T_s}$$

The mass flux $\dot{m}$ and the surface temperature T_s are obtained from the energy balance at the solid surface. For the vapor gas constant, one needs to know the molecular species in the vapor when vaporization is generated from a surface with a high-power laser. In studying the characteristics of freejet vapor expansions created by the pulse-laser vaporization of graphite materials, Covington et al.[6] have observed that the equilibrium conditions (C_3 is the predominant specie) prevail in the saturated vapor phase at high temperatures. Now that the vapor pressure is known, one can readily calculate the integrated coupling coefficient

$$C = \int_0^t P_v \mathrm{d}t \Big/ \int_0^t I \mathrm{d}t$$

Results and Discussion

The calculations have been carried out for ATJ graphite and carbon phenolic. The coupling coefficients for ATJ graphite and carbon phenolic are given in Fig. 1 as a function of time with laser intensity varying from 10^3 to 10^7 W/cm^2. We first consider the results for ATJ graphite. Before the surface temperature reaches the sublimation temperature of graphite, the coupling coefficient is negligibly small. As the surface temperature passes the sublimation temperature of graphite, the coupling coefficient rises rapidly and approaches the asympotic value of approximately 6 dyn-s/J. In order to present the preceding results in a format that can be readily compared with some actual measurements in the future, we plot the coupling coefficients as function of fluence for laser pulse times of 1, 3, and 20 μs (Fig. 2). Again, the coupling coefficients are observed to rise rapidly to the steady-state value after the appropriate levels of fluence, which correspond to the sublimation temperature, have been reached.

After the laser intensity reaches the breakdown threshold ($\sim 10^7$ W/cm^2), a plasma is ignited and a steady-state situation may eventually be attained. Basov et al.[8] have modeled the two-dimensional steady-state plasma by assuming that the plasma is a completely singly ionized gas. For the steady-state coupling coefficient with the plasma, one gets $C \approx \rho u^2 / I$, where u is the velocity at the surface. From the results of Basov et al.[8] one gets

$$C \approx 3.5 \times 10^3 (M^{7/2} / I^2 r \lambda^2)^{1/9}$$

where I is the laser intensity, r is the radius of the beam, λ is the laser wavelength, and M is the atomic weight. The coupling coefficients for the plasma with $r = 1$ cm are presented in Fig. 2.